Available online at www.sciencedirect.com
SCIENCE DIRECT
Coordination Chemistry Reviews 250 (2006) 95–109
COORDINATION CHEMISTRY REVIEWS
www.elsevier.com/locate/ccr

Review

Polymerized metallocene catalysts and late transition metal catalysts for ethylene polymerization

Jun Zhang, Xin Wang, Guo-Xin Jin *

Laboratory of Molecular Catalysis and Innovative Materials, Department of Chemistry, Fudan University, Shanghai 200433, China

Received 29 November 2004; accepted 10 June 2005
Available online 30 August 2005

Contents

Abstract

This review describes recent advances in the synthesis of novel polymerized metallocene catalysts and late transition metal catalysts for ethylene polymerization. The characteristics of these polymerized catalysts and the resulting polyethylene are discussed here.

Keywords: Metallocene; Polymerized catalysts; Late transition metal catalysts; Ethylene; Polymerization; Polyethylene

1. Introduction

In 1980, Kaminsky and co-workers [1] introduced the use of methylalumoxane (MAO) as a co-catalyst for olefin polymerization; since then metallocene complexes have revolutionized the world of polyolefins [2–4] and they are going to contribute polymers with new properties and applications.

Metallocene-based catalysts are dramatically different from previous generations of catalysts. For example, metallocene catalysts can be tailored to produce polyolefins with special stereoregularities and a high degree of tacticity. Moreover, owing to their homogeneous nature every molecule has an active site and thus metallocene catalysts can be many times more active as Ziegler–Natta and Phillips catalysts and

* Corresponding author. Tel.: +86 21 65643776; fax: +86 21 65641740.
E-mail address: gxjin@fudan.edu.cn (G.-X. Jin).

0010-8545/$ – see front matter © 2005 Elsevier B.V. All rights reserved.
doi:10.1016/j.ccr.2005.06.002

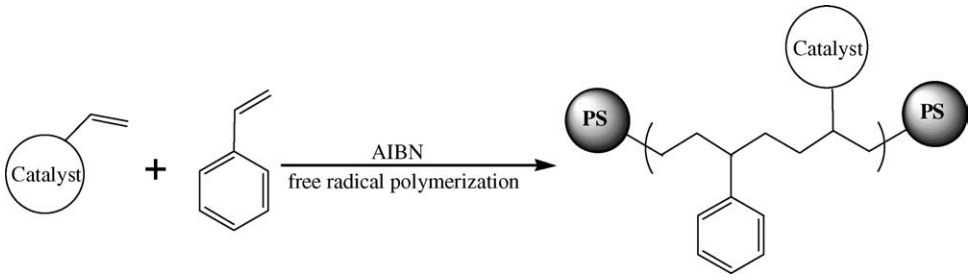

Scheme 1. Synthesis of a polymerized catalyst.

can produce high molecular weight polymers and copolymers, characterized by a narrow molecular weight distribution (≈2) and homogeneous chemical composition.

During the second half of the 1990s, interest grew in developing a new generation of late-transition metal catalysts, due to their lower oxophilicity. A greater functional-group tolerance of late transition metals relative to early transition metals was presumed, which makes them likely targets for the development of catalysts for the co-polymerization of ethylene with polar co-monomers under mild conditions. In 1995, Brookhart reported diimine nickel and Pd catalysts [5], well known for the polymerization of ethylene, α-olefins, and cyclic olefins and the co-polymerization of olefins with a variety of functionalized olefins. In 1998, Brookhart and co-workers [6] and Gibson and co-workers [7] reported highly active ethylene and propylene polymerization catalysts based on iron(II) and cobalt(II) bearing 2,6-bis(imino)pyridine ligands.

Regardless of the virtues these catalysts possess, they would remain mere playthings of the laboratory if they could not be adapted for commercial polymerization processes.

Solution polymerization processes are suitable for the preparation of low-crystallinity polyolefins, such as elastomers, very-low-density ethylene copolymers and amorphous poly-α-olefins. In these cases, the polymer product is soluble in the reaction medium and a solution-soluble catalyst system can be used. Higher-crystallinity resins, such as isotactic polypropylene or high-density polyethylene, are usually prepared in continuous slurry, fluidized-bed gas phase, or bulk monomer processes. Here, the polymer is insoluble in the reaction medium. A morphologically uniform polymer particle is needed to avoid reactor fouling and facilitate smooth operations, and thus a continuous process is possible [8]. So, it is necessary to support homogeneous catalysts for industrial applications.

Inorganic supports, such as silica or alumina [9,10], and also organic supports, such as polystyrene and starch [11,12], have been used to heterogenize soluble polymerization catalysts. These methods have the disadvantage that the catalysts can lose activity [13] because their metal centers (Lewis acids) are not accessible at the surface or they can be blocked by oxygen functions (Lewis bases). As a different heterogenization strategy, Alt et al. [14–17] developed the self-immobilization of metallocene catalysts, which have an olefin or alkyne function that can be used as a co-monomer in the polymerization process. Our group [18–21] introduced the self-immobilization of metallocene to the field of late transition metal catalysts, and Herrmann and co-workers [22] also reported on the self-immobilization of a Fe catalyst for olefin polymerization. Our group [23–26] reported a different approach that can both keep the advantages of homogeneous catalysts and improve the morphology of polymer in order to meet the requirement for industrial application. The idea was to synthesize homogeneous catalysts containing an alkenyl group on the ligand and then co-polymerize the catalysts and styrene with free radical polymerization. The resulting polymers containing catalysts as co-monomers are called polymerized catalysts (Scheme 1).

2. Preparation of precursors of polymerized metallocene catalysts

2.1. Preparation of symmetric metallocene complexes

Synthetic methods to prepare these symmetric metallocene complexes are quite general. Treatment of 2 equiv. of the ligand lithium salt with $ZrCl_4$ or $ZrCl_4$·2THF in THF affords the symmetric metallocene complexes.

The ligand lithium salt can be synthesized by two methods. One method is to treat the ligand with *n*-BuLi. Chen and Wei [27] reported two synthetic methods for alkenyl substituted cyclopentadiene, the sodium method and the phase transfer method, and the two methods were compared. When the sodium salt of cyclopentadiene reacted with allyl chloride, the yield was small. Using the phase transfer method, the yield was more than 70%. So, four new alkenyl substituted cyclopentadienes were synthesized by the phase transfer method (Scheme 2).

The other synthetic method for the ligand lithium salt is to react fulvene with lithium amide. The method was introduced by Rausch in 1982 [28]. Two ligand salts of alkenyl substituted cyclopentadienes were easily synthesized by this method (Scheme 3).

Using these ligands, the alkenyl substituted symmetrical metallocenes complexes **1**–**6** were synthesized by the reaction of 2 equiv. of the lithium salts with $ZrCl_4$ or $ZrCl_4$·2THF in THF (Scheme 4). The solid-state structure

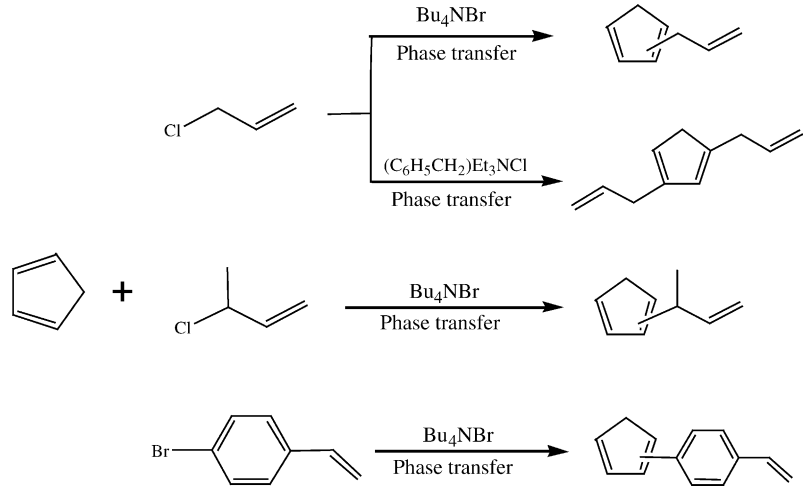

Scheme 2. Synthesis of alkenyl substituted cyclopentadiene.

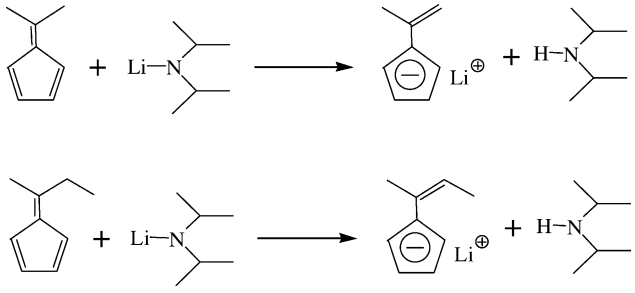

Scheme 3. Synthesis of alkenyl substituted cyclopentadienyl lithium from fulvene.

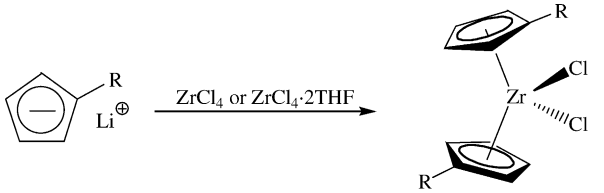

1 R: $CH_2CH{=}CH_2$
2 R: $CH_3CHCH{=}CH_2$
3 R: o-PhCH=CH_2
4 R: $CH_3C{=}CH_2$
5 R: $CH_3C{=}CHCH_3$
6 R: $(CH_2CH{=}CH_2)_2$

Scheme 4. Synthesis of alkenyl substituted symmetric metallocene dichloride complexes.

of **1** [29] was determined by X-ray crystallographic methods (Fig. 1).

2.2. Preparation of miscellaneous metallocene complexes

Dissymmetric metallocene complexes can be easily formed by the direct reaction of $Cp'ZrCl_3$ or $Cp'ZrCl_3{\cdot}DME$ with another differently substituted cyclopentadienyl or cyclopentadienyl lithium salt.

Lund and Livinghouse [30] first reported the preparation of $CpZrCl_3{\cdot}DME$. The reaction of alkenylcyclopentadienyltrimethylsilane with $ZrCl_4{\cdot}(SMe_2)_2$ in CH_2Cl_2/DME gave the alkenylcyclopentadienyl zirconium trichlorides. And then the treatment of the alkenylcyclopentadienyl zirconium trichlorides with 1 equiv. of another differently substituted cyclopentadienyl or cyclopentadienyl

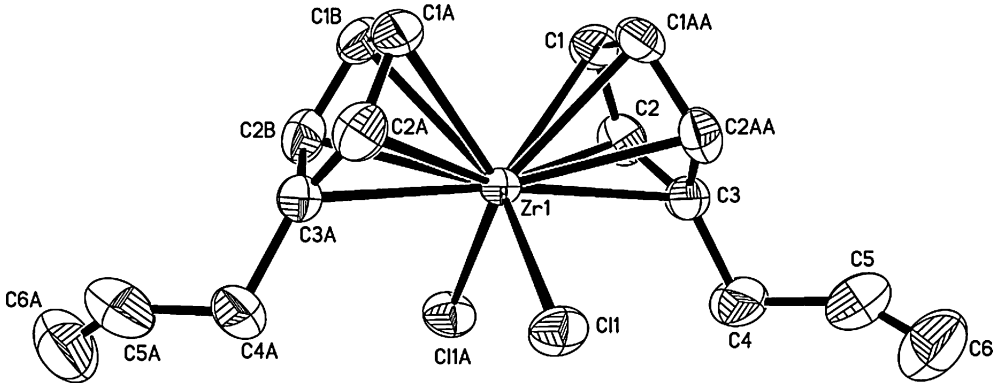

Fig. 1. Molecular structure of $[\eta^5\text{-}C_3H_5C_5H_4]_2ZrCl_2$ (**1**).

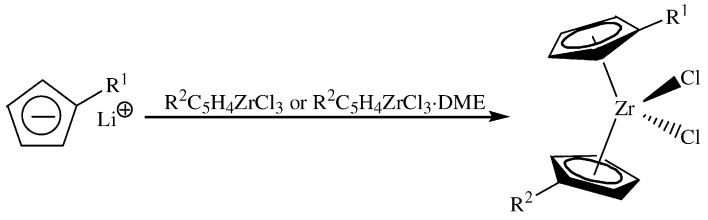

7 R^1: $CH_2CH{=}CH_2$ $R^2 = H$
8 R^1: $CH_2CH{=}CH_2$ $R^2 = (CH_3)_3C$
9 R^1: $CH_2CH{=}CH_2$ $R^2 = [(CH_3)_3C]_2$
10 R^1: o-PhCH=CH_2 $R^2 = H$
11 R^1: $CH_3C{=}CH_2$ $R^2 = H$
12 R^1: $CH_3C{=}CHCH_3$ $R^2 = H$
13 R^1: $CH_3CHCH{=}CH_2$ $R^2 = H$
14 R^1: $(CH_2CH{=}CH_2)_2$ $R^2 = H$

Scheme 5. Synthesis of dissymmetric metallocene complexes.

lithium salt led to the formation of the desired dissymmetric zirconocene complexes. The alkenylcyclopentadienyltrimethylsilane can be obtained by the reaction of the corresponding lithium salt with Me_3SiCl. Our group has employed the method to prepare alkenyl substituted dissymmetric metallocene complexes **7**–**14** (Scheme 5). The structure of **8** [29] has been determined by X-ray analysis and is characterized by the well-established distorted tetrahedron formed by two Cl atoms and two Cp rings (Fig. 2).

2.3. Preparation of silicon-bridged ansa–metallocene complexes

In general, the ansa–metallocene complexes are obtained by eliminating 2 equiv. of LiCl during the metathetical reaction of the dilithium salt of the bridged Cp ligand with MCl_4 (M = Ti, Zr, Hf).

We have [24,31,32] synthesized a series of silicon-bridged ansa–metallocene complexes containing alkenyl groups via the general synthetic route outlined in Scheme 6.

The ansa–metallocene complexes **15**–**17** were synthesized via a modified literature procedure [33]. The silylene-bridged ligand precursor was easily obtained from the allyldichloromethylsilane and cyclopentadienyl sodium. Treatment of a solution of *n*-BuLi with the bridged ligand produced the dilithium salt. The titanium complex resulted from the reaction of $TiCl_4$ with the resulting dilithium salt. The molecular structure of complex **17** [24] is presented in Fig. 3. The geometry around the Zr atom is a distorted tetrahedron formed by two Cl atoms and two Cp rings. The Zr atom, the Si atom and the two bridge-head carbon atoms are in the same plane which is nearly upright with the two C_5 ring planes.

The bridged indenyl metallocene complexes **18**–**20** were synthesized according to well-known procedures [34–37]. The indenyllithium salt was treated with the corresponding silane in diethyl ether to form the ligand precursor. Then the ligand precursor at low temperature was reacted with 2 equiv. *n*-BuLi to produce the dilithium salt. Finally, the dilithium salt was reacted with MCl_4 (M = Ti, Zr, Hf) to give the corresponding ansa–metallocene complexes.

The synthesis of complex **21** was employed through modification of methods described in the literature [38,39]. The ligand was prepared by reacting 2 equiv. fluorenyllithium salt with allyldichloromethylsilane. The bridged ligand was then converted to its corresponding zirconocene **21**. The molecular structure of **21** [32] was determined by single crystal X-ray diffraction. The geometry around the Zr atom is a distorted tetrahedron formed by two fluorenyl rings and two Cl atoms. The Zr atom, Si atom and two bridge-head carbon atoms are in the same plane (Fig. 4).

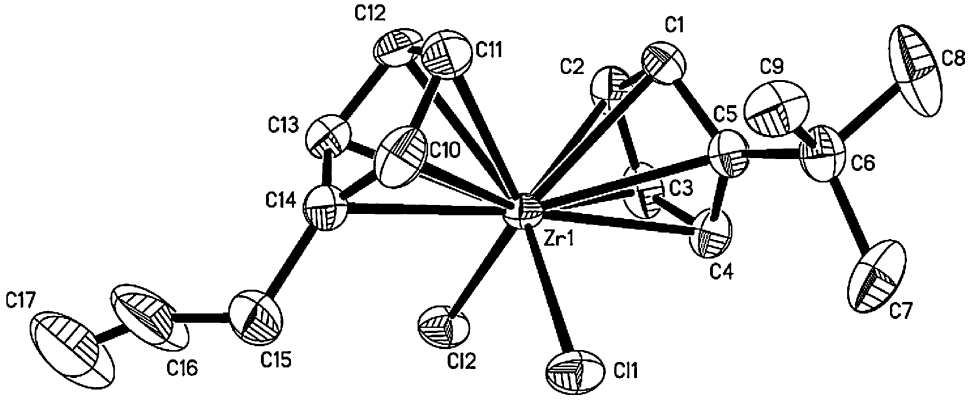

Fig. 2. Molecular structure of $(\eta^5\text{-}C_3H_5C_5H_4)(\eta^5\text{-}^tBuC_5H_4)ZrCl_2$ (**8**).

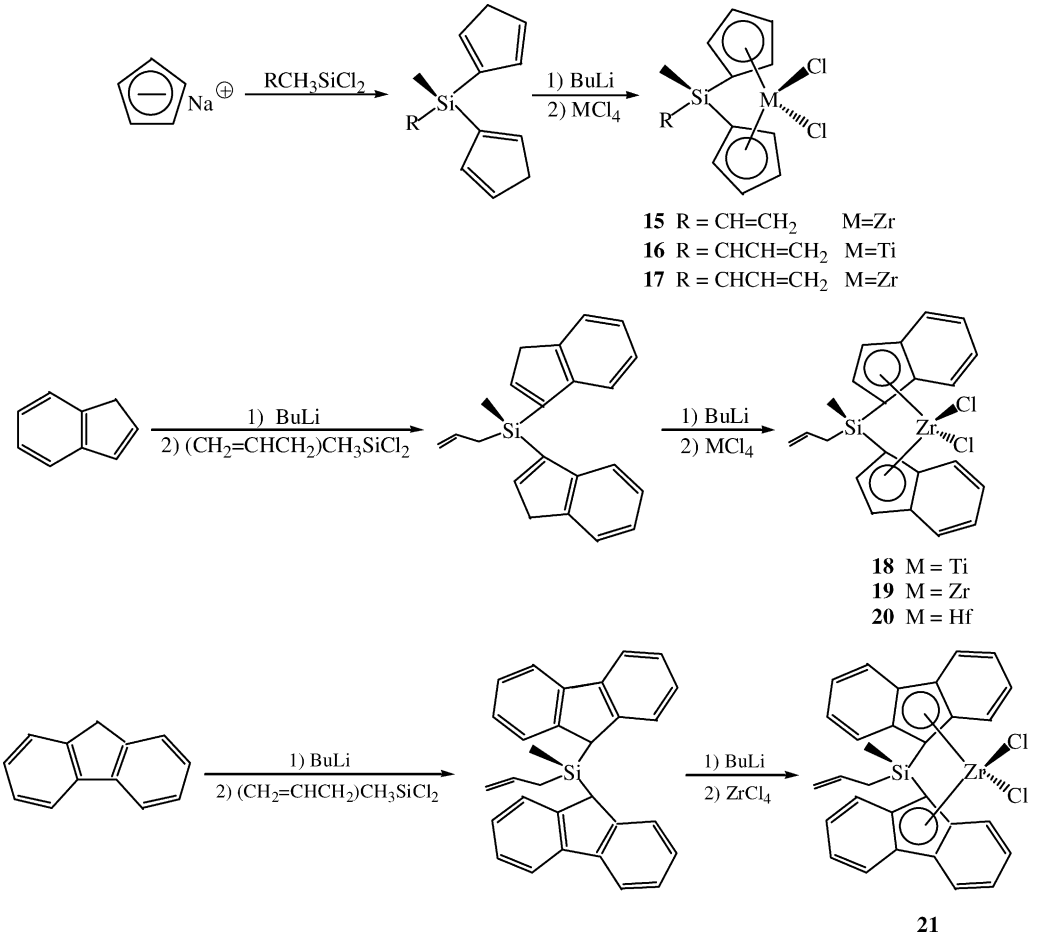

Scheme 6. Synthesis of silicon-bridged ansa–metallocene complexes.

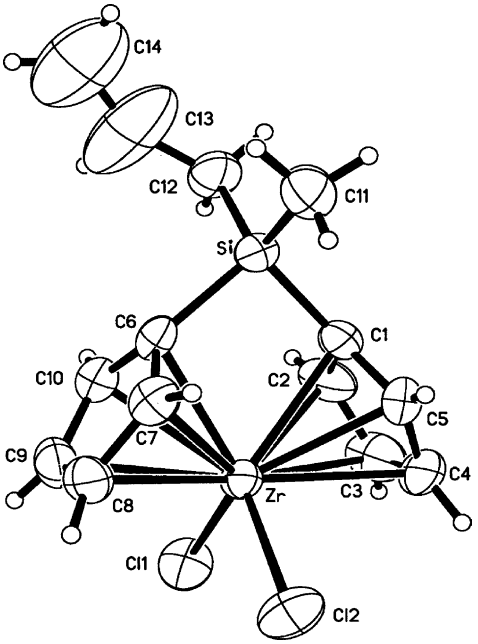

Fig. 3. Molecular structure of $[(CH_2{=}CHCH_2)CH_3Si(\eta^5\text{-}C_5H_4)_2]ZrCl_2$ (**17**) [24].

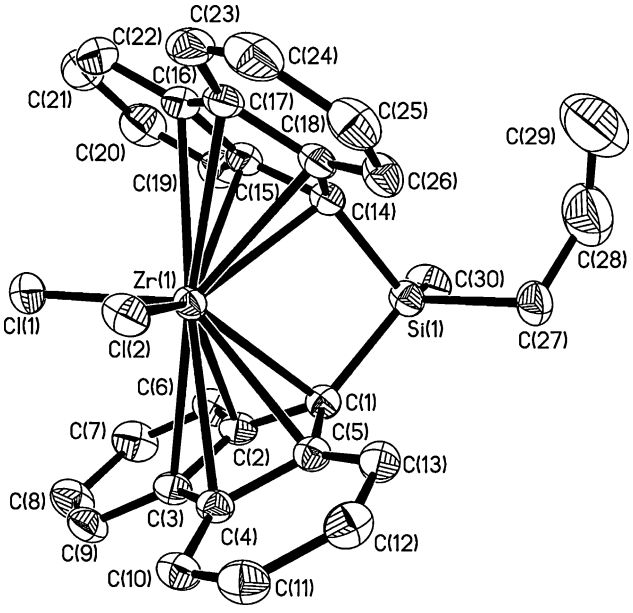

Fig. 4. Molecular structure of $C_3H_5CH_3Si(C_{13}H_8)_2ZrCl_2$ (**21**) [32].

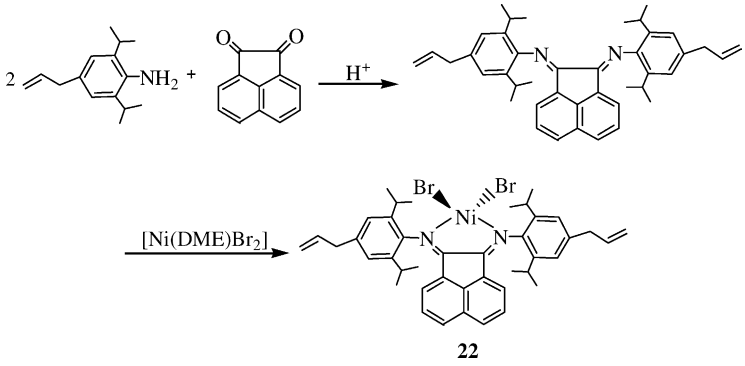

22

Scheme 7. Synthesis of diimine nickel complex **22**.

3. Preparation of precursors of polymerized late transition metal catalysts

3.1. Preparation of a diiminedibromide nickel complex

Diimine nickel complexes [5,40–42] have continued to attract much interest (Scheme 7). The steric and electronic properties of the R-diimine ligand can be readily adjusted by modifying the imino carbon and nitrogen substituents, and hence a large number of structural variations have been reported in the academic and patent literature. We [20,26] reported the synthesis of an α-diimine nickel complex bearing an allyl group. The allyl-containing imine ligand was prepared in good yield by the Schiff base condensation of allyl-substituted aniline ($Ar'NH_2$) with a carbonyl compound. Complex **22** was obtained by treatment of $Ni(DME)Br_2$ with an equivalent of *o*,*o*′-bis(4-allyl-2,6-diisopropylphenylimino) acenaphthene in CH_2Cl_2. The structure of **22** [20] (X-ray analysis) is shown in Fig. 5. The coordination geometry of **22** is a pseudo tetrahedron in which the center Ni atom is surrounded by two nitrogen atoms from the α-diimine ligand and two bromide anions. The Ni atom and N1, C1, C2, N2 form a five-membered chelate ring in complex **22**.

3.2. Preparation of bis(imino)pyridine iron complexes

The bis(imino)pyridine iron catalysts [6,7,43–45] show exceptionally high activities for ethylene polymerization, producing strictly linear, high molecular weight polymer. Our group [20,25,46,47] synthesized an analogous iron complex containing an allyl group. 2,6-Diimine pyridine complexes can be used as tridentate ligands and coordinated with $FeCl_2{\cdot}4H_2O$ in THF solution to form complexes **23**, **24** in high yield (Scheme 8).

4. Preparation of polymerized catalysts

The polymerized catalysts were prepared by the same method. The co-polymerization of styrene with a catalyst containing alkenyl group is carried out at 79–81 °C in toluene solution with AIBN as initiator in argon atmosphere. The polymerized catalyst is obtained by removing toluene under vacuum, and washed twice with a mixture of toluene and hexane. The polymerized catalysts are then re-precipitated from toluene into hexane and dried under vacuum. The composition of the polymerized catalyst is determined by ICP elementary analysis and GPC characterization.

4.1. Preparation of polymerized metallocene catalysts

We reported the polymerization of symmetric and asymmetric bis-Cp metallocene catalysts **25**–**38** [23,48] (Scheme 9). The XPS results indicated that the binding energy of metal and chloride in the polymerized metallocene catalyst **25** was a bit different from the corresponding homogeneous metallocene complex **1** (Table 1). GPC showed that the molecular weights of these polymerized metallocene catalysts were about 8000–2000, which is enough for a heterogeneous catalyst. The molecular weight distribution was 1.5–1.8. Thus, the molecular weights of the resulting polymer chains are similar as well as their lengths. Uniform composition and shape is a prerequisite for a polymer support material for a catalyst. These results show that the polymerized metallocene catalyst is a potential very useful heterogeneous catalyst for industrial applications.

We also prepared the polymerized silane bridged metallocene catalyst **39** [24] for ethylene polymerization derived from the silane bridged metallocene complex **17**. The allyl groups in **17** can be co-polymerized with styrene under radical initiator (AIBN) conditions to form the corresponding polymerized metallocene catalyst **39** (Scheme 10). In order to co-polymerize the complex with styrene sufficiently, it was necessary to control the temperature in the range of 79–81 °C. A higher temperature would lead to

Table 1
XPS results of different catalysts

	Electron binding energy (eV)	
	Zr	Cl
Cp_2ZrCl_2	181.8	198.7
1	182.3	199.1
25	182.7	199.3

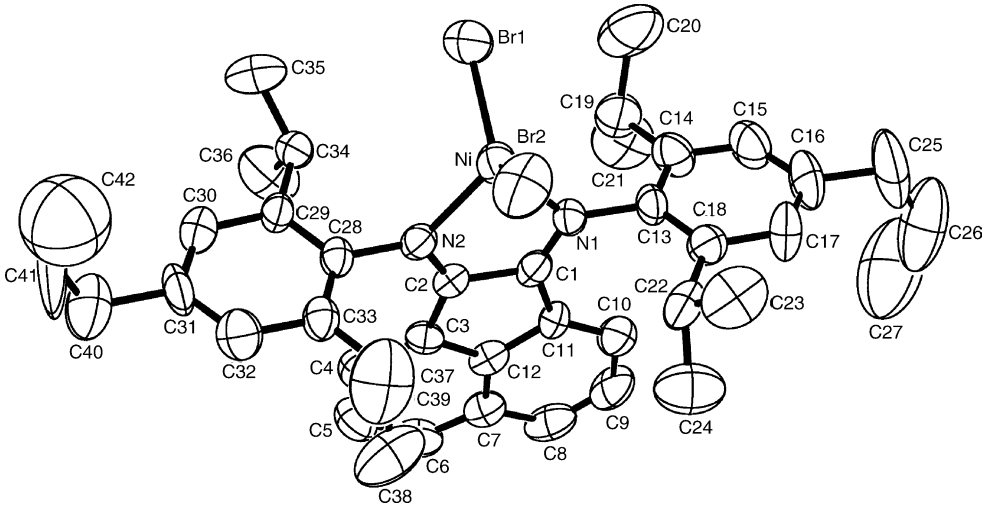

Fig. 5. Molecular structure of $[C_3H_5C_6H_2(C_3H_7)_2N]_2C_{12}H_6NiBr_2$ (**22**) [20].

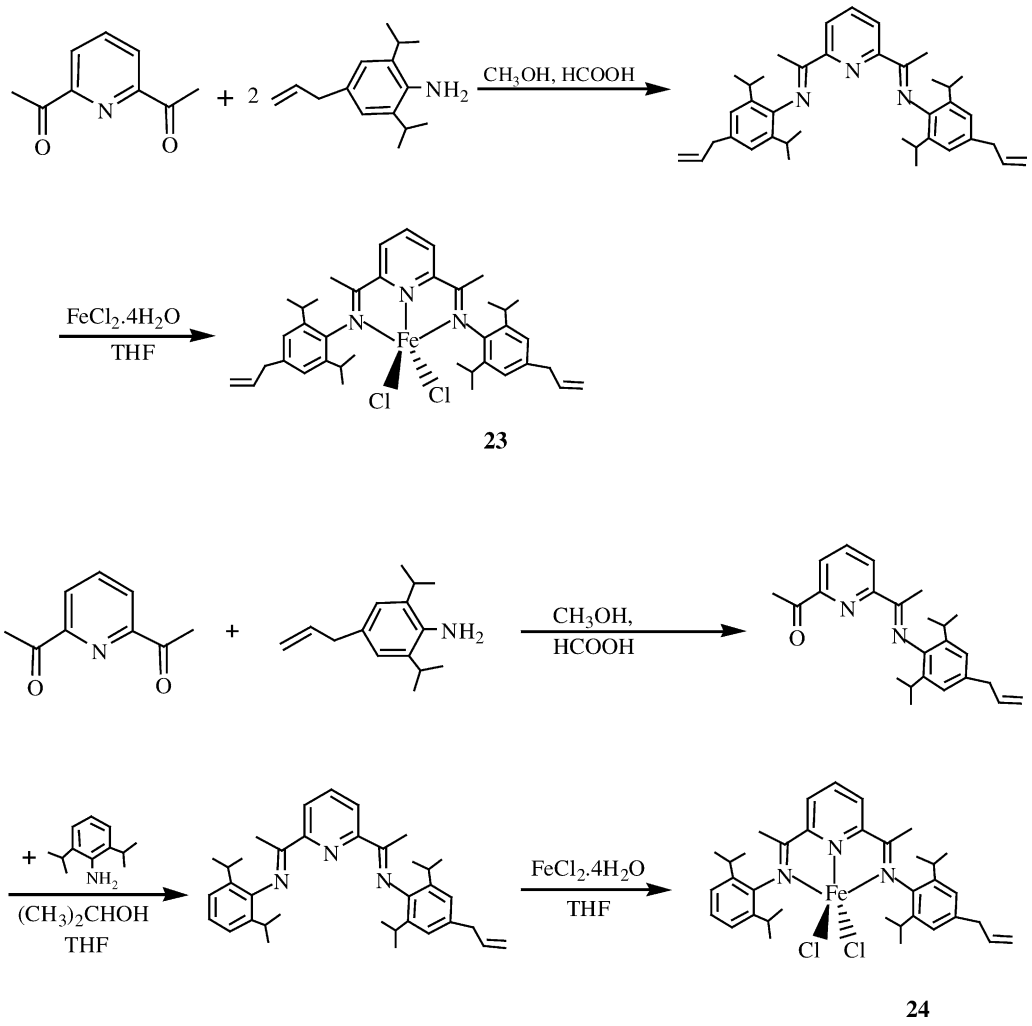

Scheme 8. Synthesis of bis(imino)pyridine iron complexes.

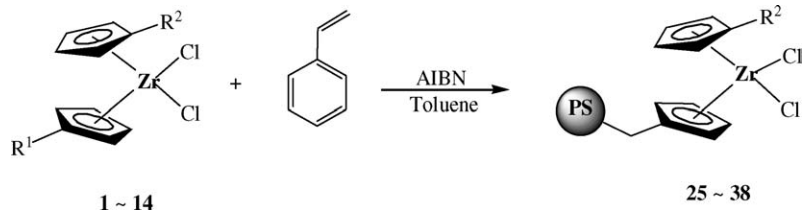

Scheme 9. Synthesis of polymerized metallocene catalysts.

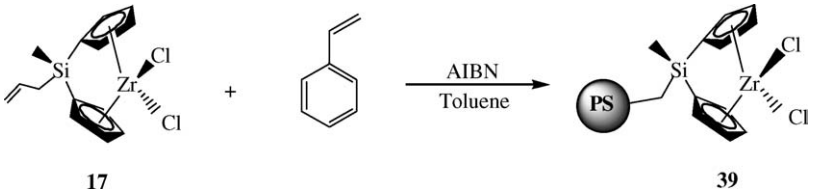

Scheme 10. Synthesis of polymerized catalyst **39**.

enhancement of the rate of homo-polymerization of styrene [49].

A GPC study of the resultant polymerized metallocene catalyst displays a molecular weight distribution no more than 1.4 (M_n = 6437; M_w = 9554; polydispersity = 1.33). The narrow MWD indicates that the length of every polymer chain is identical.

The process of the formation of the polymerized silane bridged metallocene catalyst **39** was investigated by XPS. The results show the binding energy of Si2p (101.9 eV) in **39** has a dramatic 1.2 eV increase compared to that of the corresponding catalyst **17** (100.7 eV). The XPS results confirm that the alkenyl substituent on the silicon atom has a strong interaction with styrene in the polystyrene chain. An alternative explanation is that the catalyst molecule may be imbedded in the polymer and result in the variation of the chemical surrounding of the silicon atom that can change the binding energy.

It is difficult to distinguish the structure of polymerized catalyst **39** by normal characterization methods, such as IR and ^{1}H NMR, due to the low content of the co-polymerized metallocene complex **17** in the polymer.

4.2. Preparation of polymerized late transition metal catalysts

Our group also applied the method of polymerization of the metallocene complexes to the late transition metal complexes (Scheme 11). The synthesis of polymerized α-diimine nickel catalyst **40** [26] for ethylene polymerization was performed with the α-diimine nickel complex **22**. According to these co-polymerization results (Table 2), only a small amount of monomer **22** in relation to the monomer styrene was employed, and the co-polymerizations were stopped at yields of around 45%. Higher amounts of monomer **22** or longer reaction times for higher yields can result in precipitation of copolymers insoluble in solution. Polystyrene was obtained in yields between 43.6 and 44.6%, which shows that no notable inhibition by the co-monomer **22** occurs.

IR spectra are not helpful for the determination of the functional-groups due to the low content of Ni α-diimine moieties in the polymerized catalyst **40**. In the NMR spectra, only the signal of the methyl group of isopropyl in **40** could be observed. The polymerized catalyst (PC) **40**, contained 0.018–0.049 mmol **22** moieties per g PC (1.43–3.85 wt.%). The composition of polymerized catalyst **40** in comparison to the employed **22** mixtures shows a higher reactivity of styrene (Fig. 6).

The molecular weights of polymerized catalyst **40** are of the order of $M_n \approx (8.1–8.8) \times 10^3$ and $M_w \approx (1.0–1.2) \times 10^4$. Polystyrenes obtained by homo-polymerization of styrene exhibit similar molecular weights of $M_n \approx 8.90 \times 10^3$ and $M_w \approx 1.2 \times 10^4$. Therefore, the presence of the monomer **22** does not influence the co-polymerization of styrene. No significant influence of the monomer composition on M_w was established. However, the M_w/M_n ratio decreases with

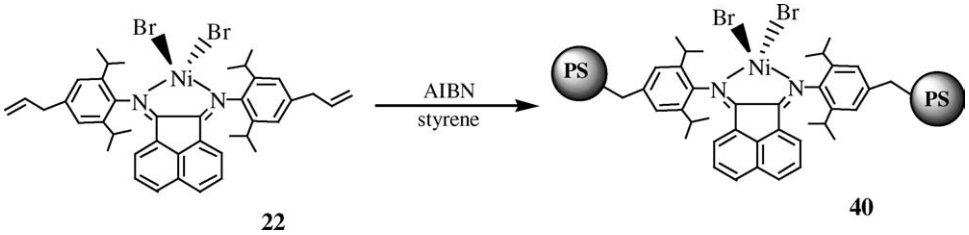

Scheme 11. Synthesis of polymerized α-diimine nickel catalyst **40**.

Table 2
Results of co-polymerizations of styrene (M_1) with monomer **22** (M_2)[a]

Entry	Mole ratio $[M_1]$:$[M_2]$ in feed	Polymer yield (g)	Mole ratio $[M_1]$:$[M_2]$ in copolymer	Content of 4 in copolymers		M_n[b] ($\times 10^3$)	M_w[b] ($\times 10^4$)	M_w/M_n[b]
				mmol/g of copolymer	wt.%			
1	–	2.34	–	–	–	8.86	1.18	1.33
2	1000	2.22	525	0.018	1.43	8.77	1.15	1.31
3	750	2.23	384	0.025	1.94	8.58	1.10	1.29
4	500	2.18	315	0.030	2.36	8.35	1.05	1.28
5	250	2.22	190	0.049	3.85	8.12	1.01	1.25

[a] Co-polymerization conditions: 50 ml of toluene; 5 g of styrene; a certain amount of **22**; 80 °C; 6 h.
[b] Determined by GPC on a Water 410 at 35 °C.

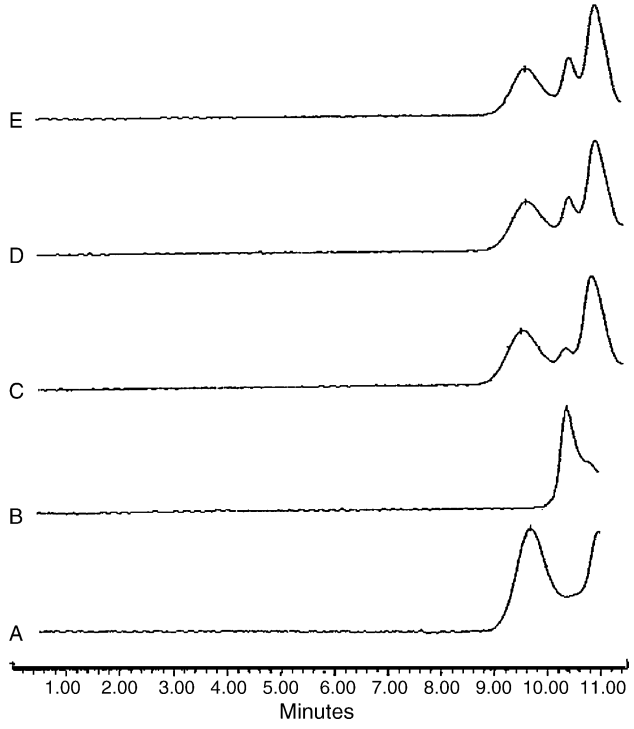

Fig. 6. GPC run of **22** (A), **40** (B) from Table 2, entry 4 and increasing mixtures of **22** and **40** (C–E).

increasing content of **22** in the monomer mixtures. This indicated that polymerized catalyst **40** with greater amounts of **22** had a narrower molecular weight distribution.

The polymerized iron catalysts **41** and **42** [25,47] prepared from the transition metal complexes **23** and **24** were also introduced (Scheme 12).

According to the results of ICP characterization, the molar ratios of starting materials (**23**: styrene and **24**: styrene) were both 1:88.3 and the corresponding copolymer unit ratios in **41** and **42** were 1:130 and 1:190. In the structure of polymerized catalysts **41** and **42**, the active center was connected to the polystyrene chains through only one or two carbon–carbon bonds. Further parallel GPC tests of three samples (B, **24**; C, **42** mixed with trace of **24**, 4.67 mg Fe/g poly.; D, **42**, 2.81 mg Fe/g poly.) were carried out. Fig. 7 shows that traces of **24** in **42** (curve C) can be distinguished by the rinsing time (10.3 min for **24**, 9.4 min for **42**). No rinsing peak appearing around 10.332 min in curve D (9.4 min for **42**, 10.9 min for THF solvent) demonstrated that the iron content in **42** (2.81 mg Fe/g poly.) is almost incorporated in polystyrene blocks. The rinsing time of the solvent THF was affected by the samples tested so that it was different in the three curves.

4.3. Preparation of shell–core polymerized catalysts

The physical shape of the catalyst influenced the physical shape of the polyethylene due to the template effect in the polymerization process. In order to improve the morphology of polymerized catalyst, our group first reported the synthesis of shell–core polymerized metallocene catalyst **43** [48]

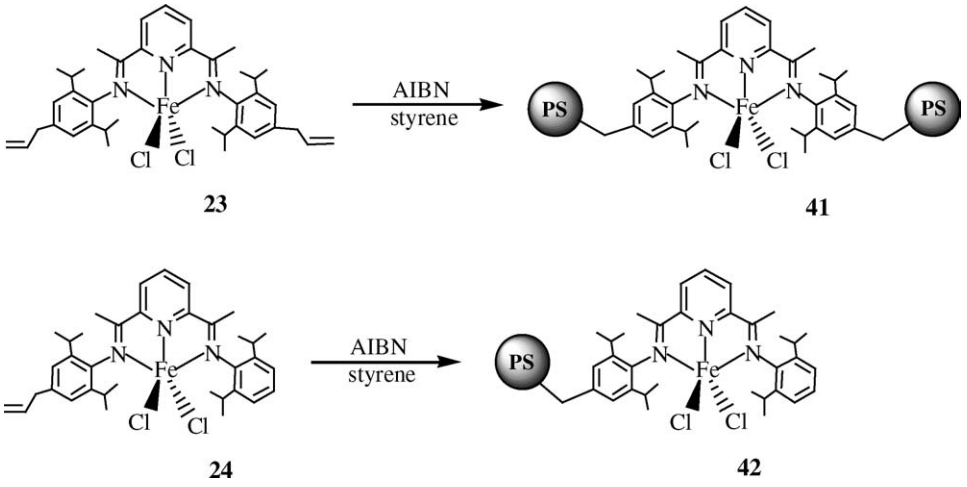

Scheme 12. Synthesis of a polymerized α-diimine nickel catalyst.

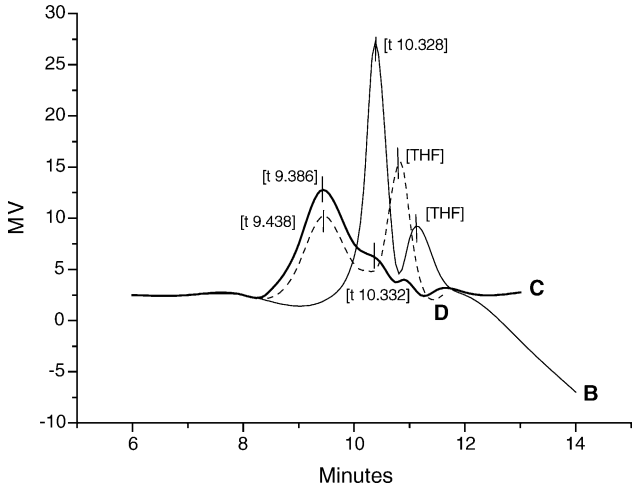

Fig. 7. The results of GPC characterization. Tests were operated on Waters 410 GPC report, injection volume: 20 μl, flow rate: 1.00 ml/min, concentration: 0.3% and int. temperature: 35 °C.

and recently succeeded in the preparation of the shell–core polymerized nickel catalyst **44** [26] and the shell–core polymerized iron catalysts **45** and **46** [25] (Fig. 8).

The mixture of SiO_2, styrene, divinylbenzene and toluene was kept at 70 °C for 30 min. Then precursor complex and initiator AIBN were added into the reaction system. The copolymerizations were carried out at 80 ± 1 °C in an argon atmosphere (Scheme 13).

The shape of **43** was spherical as showed in the SEM image (Fig. 9). The center of catalyst was SiO_2, while the soft substance surrounding SiO_2 was the polystyrene containing the polymerized metallocene complex with low cross-linking degree.

The cross-linking degree of the resulting polystyrene plays an important role in the preparation of the shell–core polymerized catalysts. The catalysts with high cross-linking degree are insoluble in toluene and cannot cover around the surface of SiO_2 beads well. Whereas, for the shell–core

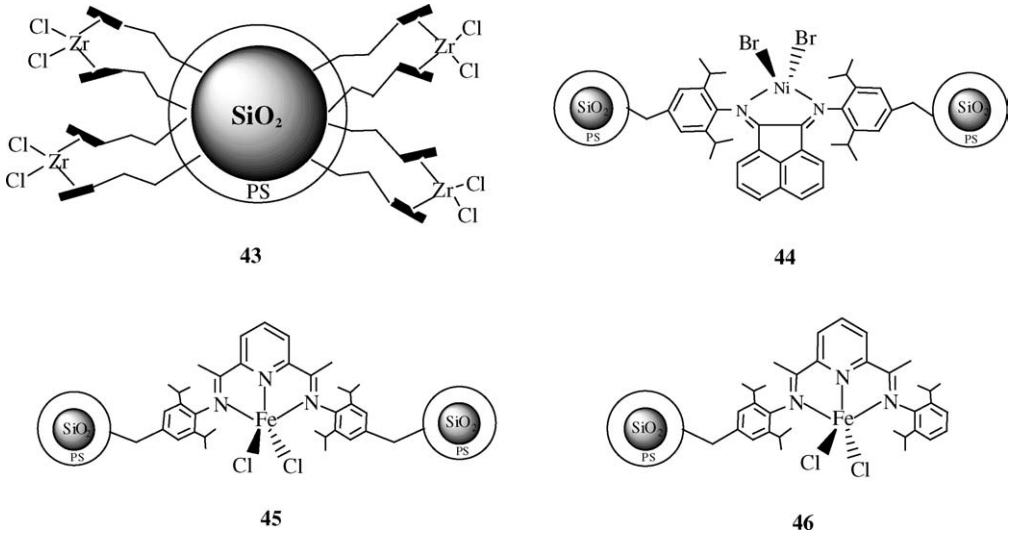

Fig. 8. Shell–core polymerized catalysts **43**, **44**, **45**, and **46**.

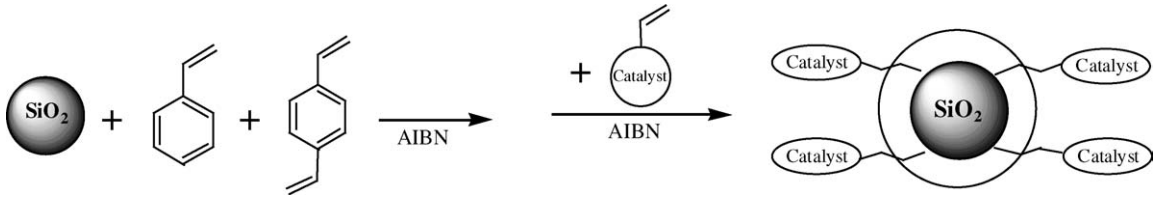

Scheme 13. Synthesis of shell–core polymerized catalysts.

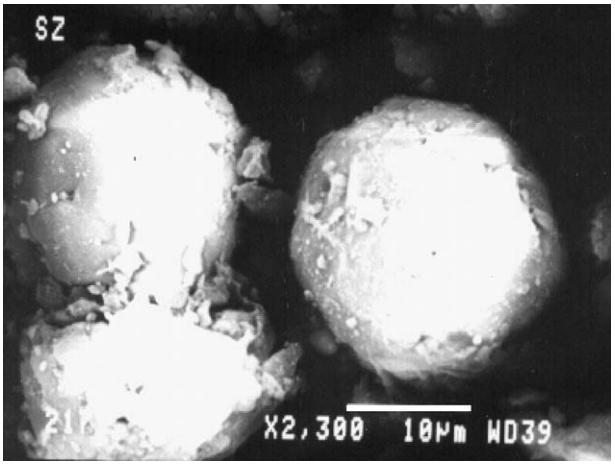

Fig. 9. SEM image of a shell–core polymerized metallocene catalyst.

polymerized catalysts with too low cross-linking degree, they will be frail and easy to disintegrate because of the swelling effect of the polystyrene in toluene. The shell–core polymerized iron catalyst **45** has a cross-linking degree of 4.07% (calculated according to the starting materials).

5. Polymerization of ethylene

Polymerized catalysts show high activities for ethylene polymerization, in some cases even higher than their homogeneous counterparts. Other supported heterogeneous catalysts have only one half or a tenth of the activity of their homogeneous counterparts [11,50]. This is indicative that the catalyst centers are not deactivated or partially blocked in the polymerization process. Scheme 14 describes the proposed mechanism for the ethylene polymerization catalyzed by polymerized metallocene catalysts. The metallocene complexes are incorporated in the polystyrene chains, and when activated by MAO, the active centers are distributed over the polymer chain preventing the loss of activity.

Table 3
Results of ethylene polymerization under high pressure

Catalyst	**40**
Activity ($\times 10^7$ g PE/(mol Zr h))	6.48
Bulk density (g/cm^3)	0.341
M_w	167000
M_w/M_n	2.7
Density (g/cm^3)	0.917
Melting point (°C)	128.2
ΔH_m	38.7 cal/g,159.4 J/g

Conditions:1.4 MPa, 70 °C.

The polymerized metallocene catalysts **25**–**38** activated with MAO show activities in the range of $(3–5) \times 10^6$ g PE/(mol Zr h). Their activities were higher than in homogeneous solution without the co-polymerization of styrene. Obviously, the polymerized metallocene catalysts have dispersed active sites and avoid deactivation. Using catalyst **25**, high molecular weight polymers ($M_v = 2.31 \times 10^5$) with T_m (136.1 °C) were obtained.

Under high pressure, the shell–core catalyst **40** showed high activity for ethylene polymerization (Table 3). The molecular weight of polyethylene was about 167,000. The bulk density of the produced polyethylene was about 0.341. Thus, this kind of catalysts has potential use for industrial application.

The performance of the catalysts **17** and **39** was evaluated on the basis of ethylene polymerization in toluene [24]. Table 4 compares the polymerization productivity of **17** with **39** at identical conditions. The data show that the increment of Al/Zr (molar ratio) leads to great increase in activity, but extreme concentration of MAO may hinder the ethylene insertion, making the active centers embedded and useless, and thus the activity decrease. The polymer immobilized

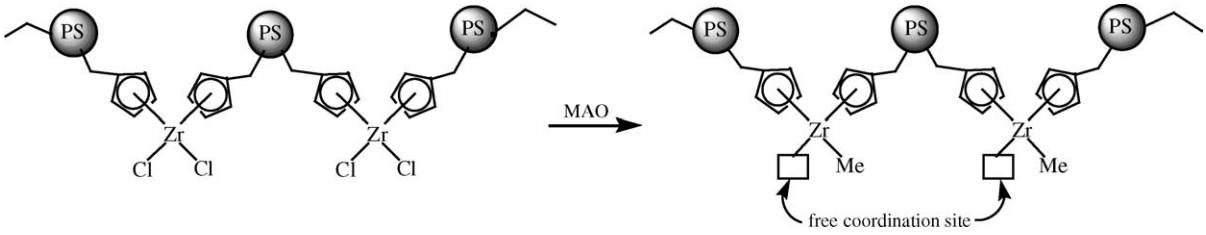

Scheme 14. Possible mechanism for the ethylene polymerization catalyzed by polymerized catalysts.

Table 4
Ethylene polymerization with catalysts **17** and **39** [24]

Entry	Polymerization conditions			Productivity (10^5 g PE/(mol Zr h))	
	T (°C)	[Al]/[Zr] (molar ratio)	[Zr] ($M \times 10^{-6}$)	Catalyst **17**	Catalyst **39**
1	25	1100	2.0	1.05	4.23
2	25	1650	2.0	1.65	4.80
3	25	2200	2.0	4.15	5.05
4	25	2750	2.0	1.50	8.74
5	25	3300	2.0	1.40	2.45
6[a]	25	1500		3.73 [13a]	
7[b]	50	200			1.72[13b]

[a] Cp_2ZrCl_2 as catalyst [51].
[b] Cp_2ZrCl_2 supported in the SiO_2 as catalyst [52].

metallocene **39** are found to be more active than **17**. The mechanistic explanation is that the fixation of the catalyst molecule on the polymer chain may reduce the bimolecular deactivation, improving the activity of **39**.

The DSC results (T_m = 130.1 °C, T_c = 115.0 °C) show that the PE produced by **39** has high crystallinity (>70%), resulting from the highly linear structure of PE. The GPC data (M_w = 60,500, M_n = 12,800, M_w/M_n = 4.7) suggest that the active species formed in the polymer immobilized catalyst are not uniform. The origin of the behavior is not clear at present. Both metal species with different environment and access to the substrate can play a certain role.

The polymerized nickel catalysts **40** and **44** were also found to show high activities for ethylene polymerization when activated with MMAO [26]. The results of ethylene polymerization tests using these iron catalysts are exhibited in Table 5.

The feasible Al/Ni ratio of catalyst **22** was lower than that of **40** and **44**. However, catalyst **44** was found to display a higher polymerization activity at 25 °C and **22** and **40** did so at 0 °C, which indicated that, after being supported on SiO_2, the shell–core polymerized catalyst **44** better met the needs of the industrial process than **22** and **40**. With increasing ethylene pressure, catalysts **40** and **44** showed higher activities ((5.74 and 6.92) × 10^6g PE/(mol Ni h) at 0.4 MPa).

The number average molecular (M_n) values of polyethylene produced by **44** ranged from 171,000 to 179,000 (from 130,000 to 207,000 by **40** and from 111,000 to 222,000 by **22**) and M_w/M_n value is from 2.296 to 2.401 (from 2.034 to 2.144 by **40** and from 1.767 to 2.274 by **22**), which suggested that polymerization temperature had little influence on the molecular weight or on the molecular weight distribution of polymer products activated by the shell–core polymerized catalyst **44**.

Since the spherical supported SiO_2 core could increase the rigidity of the catalyst beads and give a suitable template, the polymer particles produced by catalyst **44** replicated the morphological characters of the starting particles of the shell–core catalyst and afforded spherical polyethylene particles (Fig. 10).

The chemical shifts in the ^{13}C NMR spectra of the polyethylenes catalyzed by catalysts **22**, **40** and **44** are given in Table 6. Alkyl branches were identified by resonances at 30.1(CH_2), 20.1(CH_3), 33.5(CH), 37.8(α-CH_2), 27.6(β-CH_2), 30.5 ppm (γ-CH_2), which were confirmed over the entire spectrum [19,53,54]. Alkyl branches were estimated

Table 5
Results of ethylene polymerization [26]

Entry	Catalysts	T (°C)	Al/Ni (molar ratio)	Activity (10^6 g PE/(mol Ni h))	M_n[a]	M_w[a]	M_w/M_n[a]
1	**22**	25	2500	2.67	111000	196000	1.767
2		0	2500	3.32	194000	479000	2.472
3		−15	2500	2.83	222000	504000	2.274
4	**40**[b]	25	3500	1.80	130000	264000	2.034
5		0	3500	2.62	177000	472000	2.661
6		−15	3500	1.50	207000	444000	2.144
7[c]		–	3500	5.74	n.d.	n.d.	n.d.
8	**44**	25	3000	1.11	171000	393000	2.296
9		0	3000	0.86	178000	434000	2.434
10		−15	3000	0.36	179000	430000	2.401
11[d]		–	3000	6.92	n.d.	n.d.	n.d.

Polymerization condition: All of the catalysts (1.0 μmol) were activated with MMAO; 30 min of polymerization time; 50 ml of toluene; 0.1 MPa of ethylene pressure.
[a] Determined by GPC at 150 °C.
[b] **40** from Table 2 entry 4.
[c] 4.0 μmol catalyst **40**; 0.4 MPa of ethylene pressure; 20 min without temperature control of polymerization time.
[d] 3.26 μmol catalyst **44**; 0.4 MPa of ethylene pressure; 15 min without temperature control of polymerization time.

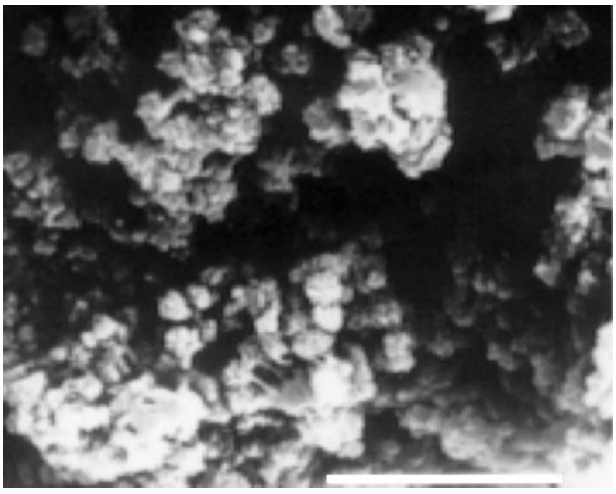

Fig. 10. SEM image of polyethylene beads resulting from catalyst **44** (scale bar, 10 μm).

with 14, 13 and 26 branches per 1000 carbons. No other kinds of short branches can be observed through this ^{13}C NMR research. The similar microstructures of polyethylene showed that both polymerized catalyst **40** and polymerized shell–core catalyst **44** all kept the same coordinate circumstances surrounding the active center as the original monomer catalyst **22**.

The DSC results of catalysts **22**, **40** and **44** indicate that these catalysts converted ethylene to linear polyethylene with low crystallinity (≤30%). Melting temperatures (T_m (°C)) of produced polyethylene are 117 °C (**44**), 116 °C (**40**) and 105 °C (**22**), indicative of high-density polyethylene.

The polymerized iron catalysts **41**, **42**, **45** and **46**, as well as the homogeneous catalysts **23** and **24** exhibit high activities using modified methylaluminoxane (MMAO) as a co-catalyst [25]. The results of ethylene polymerization tests using these iron catalysts are collected in Table 7.

Different from the cases of catalysts **23** and **24**, the ethylene polymerization catalyzed by catalysts **41** and **42** proceeds smoothly without an immediate exotherm and a decrease in activity. The dispersion of iron complexes among polystyrene blocks refrained from the too high

Table 6
^{13}C NMR spectroscopic data of polyethylenes resulting from the nickel catalysts [26]

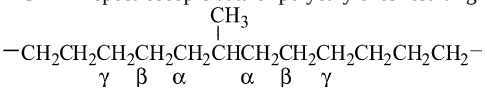

Catalyst	δ (CH_2) (ppm)	δ (CH_3) (ppm)	δ (CH) (ppm)	δ (α-CH_2) (ppm)	δ (β-CH_2) (ppm)	δ (γ-CH_2) (ppm)	Branches per 1000 carbons
22 (Table 5, entry 2)	30.15	20.14	33.51	37.79	27.63	30.53	14
40 (Table 5, entry 5)	30.15	20.10	33.51	37.79	27.63	30.53	13
44 (Table 5, entry 9)	30.11	20.06	34.85	37.75	27.59	30.53	26

Table 7
Results of ethylene polymerization [25]

Entry[a]	Catalyst	T (°C)	Pressure (MPa)	Al/Fe (molar ratio)	Activity (10^6 g PE/(mol Fe h))	Molecular weight		
						M_w[b]	M_n[b]	M_w/M_n[b]
1	**23**	25	0.1	1600	1.59	142000	3000	47.42
2		0	0.1	1600	1.90	187000	9000	21.45
3	**24**	13	0.1	2200	1.59	90000	1000	92.62
4		0	0.1	2200	4.02	180000	8000	23.13
5	**41**	25	0.1	1200	0.37	–	–	–
6		25	0.1	1600	0.43	100000	1000	68.64
7		60	0.24	1600	3.13	182000	7000	27.09
8	**42**	13	0.1	1650	2.23	–	–	–
9		13	0.1	2200	2.47	129000	3000	47.38
10		60	0.24	2200	3.90	154000	7000	23.58
11	**45**	51	0.1	1200	0.67	31.2×10^4[c]		
12		60	0.3	1200	3.09	25.5×10^4[c]		
13		51	0.3	1200	2.51	94.0×10^4[c]		
14	**46**	51	0.1	1600	1.09	30.6×10^4[c]		
15		60	0.3	1600	3.18	28.1×10^4[c]		
16		51	0.3	1600	2.62	87.0×10^4[c]		

Polymerization condition: All of the catalysts activated with MMAO; 1 h of polymerization time.

[a] Entries 1–10, 50 ml of toluene solvent; entries 11, 13, 14, 16, 100 ml of hexane solvent; entries 12, 15, 100 ml of toluene solvent.

[b] Determined by GPC at 135 °C.

[c] Polymer did not dissolve completed in trichlorobenzene under GPC measurement conditions. The results were obtained from the polyethylene soluble in decalin under intrinsic viscosity measurement conditions.

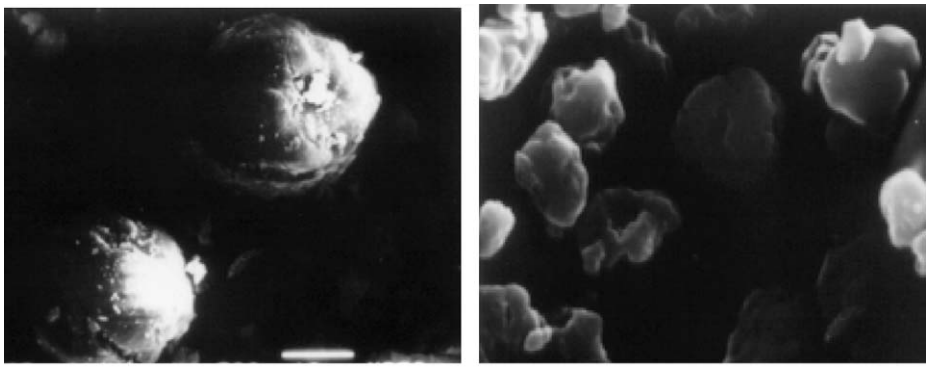

Fig. 11. (A) Scanning electron microscope image of the **45** particle (scale bar, 10 μm); (B) scanning electron microscope image of the polyethylene bead resulted from the **45** catalyst at 60 °C and 0.3 MPa of ethylene pressure (scale bar, 10 μm).

concentration of active center in the polymerization system and promised the ethylene polymerization in a smooth pace. As a result, **41** was found to display an activity of 4.3×10^5 g PE/(mol Fe h) at 25 °C which was lower than the activity of ethylene polymerization catalyzed by **23** at the same polymerization conditions (1.59×10^6 g PE/(mol Fe h)). However, **42** was found to display a higher activity than that of **24** at the same polymerization conditions (at 13 °C, **42**: 2.47×10^6 g PE/(mol Fe h); **24**: 1.59×10^6 g PE/(mol Fe h)). The different polymer configuration of the polymerized catalysts **41** and **42** may contribute to this observation.

Although the polymer-incorporated iron catalysts **41** and **42** are active for ethylene polymerization and avoid immediate exotherm, the morphology of the polyethylene catalyzed by **41** and **42** is a little poor, with particles of varied and ill-defined shapes.

The shell–core polymerized catalysts **45** and **46** exhibited high activities because fewer active centers were enwrapped in inner spherical articles. Catalyst **45** showed a very high activity of 3.08×10^6 g PE/(mol Fe h) at 60 °C and 0.3 MPa of ethylene pressure with a viscosity average molecular weight (M_v) value of 25.47×10^4 and the catalyst **46** was found to display a very high activity of 3.18×10^6 g PE/(mol Fe h) at 60 °C and 0.3 MPa of ethylene pressure with a viscosity average molecular weight (M_v) value of 28.13×10^4. Most excitingly was that the shell–core polymerized iron catalysts **45** and **46** gave unexpectedly high molecular weight polyethylene. The polyethylene with very high viscosity average molecular weight (M_v) value of 93.97×10^4 was obtained at 51 °C by using **45** as catalyst, and the polyethylene with a viscosity average molecular weight (M_v) value of 86.98×10^4 was obtained at 51 °C by using **46** as catalyst. In comparison, **42**/MAO provided the polyethylene with a viscosity average molecular weight (M_v) value of 18.2×10^4 at 60 °C and 0.24 MPa of ethylene pressure [47], and 2,6-diacetylpyridine bis(2,6-diisopropylanil) iron dichloride reported by Gibson provided polyethylene with molecular weight (M_w) value of 2.76×10^4 at 60 °C and 1.33 MPa ethylene pressure [7]. The explanation of such results is not clear.

The SiO_2 core strengthens the rigidity of the catalysts beads and affords the suitable spherical mode for polyethylene products. The polyethylene resulting from **45** and **46** was isolated in the form of discrete spherical beads (Fig. 11).

All these iron catalysts produce essentially linear polyethylenes with broad molecular weight distribution. Bimodality of polyethylene is attributed to the additional chain termination mechanism (chain transfer to aluminum), which predominates at high concentrations of the aluminoxane activator and at short reaction times. ^{13}C NMR analyses of the polyethylenes generated by all those iron catalysts reveal that resonances at 14.1, 22.85, 29.57, 29.69 and 32.21 ppm are obvious in all tests, by which the saturated end group in the polymer chains is identified. This end groups arise from chain transfer to aluminum followed by hydrolysis during the acidic workup [44].

6. Summary and outlook

This review highlights the polymerization of polymerized metallocene and late transition metal catalysts, which provides an elegant technology to immobilize homogeneous catalysts. The polymerized catalysts described herein not only kept the advantage, such as high activities, of the original homogeneous catalysts but also improved the particle morphology and thus bulk density of polyethylene products because of the template-effect of the supported catalysts. This new method for the immobilization of olefin catalysts makes it possible to apply homogeneous catalysts in industrial gas phase or slurry reactors as heterogeneous catalysts. Consequently, taking benefit of this feature, the polymerization technology of homogeneous catalysts could be applied to some other catalyst systems, such as Fujita's FI catalyst.

Acknowledgements

Financial support by the National Science Foundation of China for Distinguished Young Scholars (29925101, 20274008) and by the special Funds for Major State Basic Research Projects (2005CB623800) is gratefully acknowledged.

References

[1] (a) H. Sinn, W. Kaminsky, H.J. Vollmer, R. Woldt, Angew. Chem. Int. Ed. Engl. 19 (1980) 396;
(b) W. Kaminsky, J. Chem. Soc. Dalton Trans. (1998) 1413;
(c) H.G. Alt, A. Köppl, Chem. Rev. 100 (2000) 1205.
[2] K.B. Sinclair, R.B. Wilson, Chem. Ind. (1994) 857.
[3] (a) W.-W. du Mont, M. Weidenbruch, A. Grochman, M. Bochmann, Nachr. Chem. Tech. Lab. 43 (1995) 115;
(b) G. Erker, Chem. Comm. (2003) 1469.
[4] R. Beckhaus, Nachr. Chem. Tech. Lab. 46 (1998) 611.
[5] L.K. Johnson, C.M. Killian, M. Brookhart, J. Am. Chem. Soc. 117 (1995) 6414.
[6] B.L. Small, M. Brookhart, A.M.A. Bennett, J. Am. Chem. Soc. 120 (1998) 4049.
[7] G.J.P. Britovsek, V.C. Gibson, B.S. Kimberley, P.J. Maddox, S.J. McTavish, G.A. Solan, A.J.P. White, D.J. Williams, Chem. Commun. (1998) 849.
[8] K. Kallio, U. Palmqvist, H. Knuuttilla, A.M. Fatnes, PCT Int. Appl. 96 (1996) 34898.
[9] K. Soga, M. Kaminaka, Macromol. Chem. Rapid Commun. 12 (1991) 367.
[10] K. Soga, M. Kaminaka, Macromol. Chem. Rapid Commun. 13 (1992) 221.
[11] G.G. Hlatky, Chem. Rev. 100 (2000) 1347.
[12] T.R. Boussie, C. Coutard, H. Turner, V. Murphy, T.S. Powers, Angew. Chem. 110 (1998) 3472.
[13] W. Kaminsky, M. Arndt, Adv. Polym. Sci. 127 (1997) 143.
[14] H.G. Alt, J. Chem. Soc. Dalton Trans. (1999) 1703.
[15] H.G. Alt, M. Jung, J. Organomet. Chem. 580 (1999) 1.
[16] A. Koeppl, H.G. Alt, J. Mol. Catal. A: Chem. 165 (2001) 23.
[17] A. Licht, H.G. Alt, J. Organomet. Chem. 648 (2002) 134.
[18] D. Zhang, G.-X. Jin, N.H. Hu, Chem. Commun. (2002) 574.
[19] D. Zhang, G.-X. Jin, N.H. Hu, Eur. J. Inorg. Chem. (2003) 1570.
[20] (a) D. Zhang, G.-X. Jin, J. Polym. Sci., Polym. Chem. 42 (2004) 1018;
(b) S. Guo, D. Zhang, G.-X. Jin, Chin. Sci. Bull. 49 (2004) 249;
(c) S. Guo, G.-X. Jin, F. Wang, J. Polym. Sci., Polym. Chem. 42 (2004) 4830.
[21] D. Zhang, G.-X. Jin, Appl. Catal. A: Gen. 262 (2004) 85.
[22] F.A.R. Kaul, G.T. Puchta, H. Schneider, F. Bielert, D. Milalios, W.A. Herrmann, Organometallics 21 (2002) 74.
[23] G.Y. Zhou, G.-X. Jin, Advances on Organometallic Catalysts and Olefin Polymerization in China and Germany, Chemical Industry Press, Beijing, 2001, pp. 173–183.
[24] H.B. Zhu, G.-X. Jin, N.H. Hu, J. Organomet. Chem. 655 (2002) 167.
[25] C.K. Liu, G.-X. Jin, New J. Chem. 26 (2002) 1485.
[26] (a) D. Zhang, G.-X. Jin, Appl. Catal. A: Gen. 262 (2004) 13;
(b) D. Zhang, G.-X. Jin, Organometallics 22 (2003) 2851;
(c) D. Zhang, G.-X. Jin, F.S. Wang, Organometallics 23 (2004) 3270.
[27] S.S. Chen, R.B. Wei, Chin. Sci. Bull. 15 (1983) 921.
[28] D.W. Macomber, W.P. Hart, M.D. Rausch, J. Am. Chem. Soc. 104 (1982) 884.
[29] J. Zhang, Ph.D. Dissertation, Fudan University, 2004.
[30] E.C. Lund, T. Livinghouse, Organometallics 9 (1990) 2426.
[31] H.B. Zhu, G.-X. Jin, Acta Chim. Sin. 60 (2002) 509.
[32] G.R. Tang, G.-X. Jin, L.H. Weng, J. Organomet. Chem. 689 (2004) 678.
[33] T. Hunh, N. Suzuki, Y. Yamaguchi, T. Mise, T. Chihara, Y. Wakatsuki, Chem. Lett. 12 (1997) 1201.
[34] W.A. Herrmann, J. Rohrmann, E. Herdtweck, W. Spaleck, A. Winter, Angew. Chem. Int. Ed. Eng. 28 (1989) 1511.
[35] W. Spaleck, J. Rohrmann, A. Winter, B. Bachmann, P. Kipof, J. Behm, W.A. Herrmann, Angew. Chem. Int. Ed. 31 (1992) 1347.
[36] H.G. Alt, M. Jung, J. Organomet. Chem. 562 (1998) 229.
[37] H.G. Alt, M. Jung, J. Organomet. Chem. 568 (1998) 87.
[38] E.J. Thomas, M.D. Rausch, J.C.W. Chien, Organometallics 19 (2000) 4077.
[39] B. Peifer, W. Milius, H.G. Alt, J. Organomet. Chem. 553 (1998) 205.
[40] A.C. Gottfried, M. Brookhart, Macromolecules 34 (2001) 1140.
[41] O.I.R. Neto, R.S. Mauler, R.F. De Souza, Macromol. Chem. Phys. 202 (2001) 3432.
[42] L.C. Simon, R.S. Mauler, R.F. De Souza, J. Polym. Sci. Polym. Chem. 37 (1999) 4656.
[43] V.C. Gibson, D.F. Wass, Chem. Br. 7 (1999) 20.
[44] A.M.A. Bennett, Chemtech 29 (1999) 24.
[45] G.J.P. Britovsek, M. Bruce, V.C. Gibson, B.S. Kimberley, P.J. Maddox, S. Mastroianni, S.J. McTavish, C. Redshaw, G.A. Solan, S. Stromberg, A.J.P. White, D.J. Williams, J. Am. Chem. Soc. 121 (1999) 8728.
[46] C.K. Liu, G.-X. Jin, Chem. J. Chin. Univ. 22 (2001) 1233.
[47] C.K. Liu, G.-X. Jin, Acta Chim. Sin. 60 (2002) 157.
[48] G.Y. Zhou, Ph.D. Dissertation, Changchun Institute of Applied Chemistry, Chinese Academy of Sciences, 1999.
[49] G.-X. Jin, G.Y. Zhou, Y. Liu, Chinese Patent 98,125,651.
[50] P.J.T. Tait, M.G.K. Monteiro, M. Yang, J.L. Richardson, Proceedings of MetCon 1996, Houston, TX, June, 12–13, 1996.
[51] F. Ciardeli, A. Altomare, G. Arribas, in: K. Soga, M. Terano (Eds.), Catalyst Design for Tailor-Made Polyolefin, Elsevier, Amsterdam, 1994, p. 257.
[52] M.C. Sacchi, D. Zucchi, I. Tritto, P. Locatelli, Macromol. Rapid Commun. 16 (1995) 581.
[53] L.P. Linderman, N.O. Adams, Anal. Chem. 43 (1971) 1245.
[54] D.E. Dorman, Macromolecules 5 (1972) 574.